

Theoretical Models, Preparation, Characterization and Applications of Cyanine J-Aggregates: A Minireview

Nitzan Dar* and Rinat Ankari^[a]

Cyanines are one of the few kinds of molecules whose absorbance and emission can be shifted in a broad spectral range from the ultraviolet to the near infrared. They can easily transform into J-aggregates with narrow absorption and emission peaks, along with a redshift in their spectra. This minireview presents cyanine dyes and their J-aggregates and

discusses their structure and spectral properties that illustrate their specificities. We summarize the theoretical and experimental state of the art on cyanine J-aggregates and their applications, also laying the groundwork for cyanine J-aggregates synthesis and characterization methods.

1. Introduction

Cyanine dyes and their J-aggregates (Cyanine J-aggregates, [CJA]) are a fascinating topic for both basic and applied science. Many efforts have been made to study the mechanism behind the aggregation of these dyes, and the vast range of their properties still attracts attention. The cyanine dye family is based on compounds with a polymethine chain of various lengths. These chains contain a single positively charged nitrogen atom, usually as part of a heterocycle, which is surrounded by a counter anion (Figure 1). As a result of this structure, these molecules have a high absorption coefficient and fluorescence emission intensity. One of the most interesting properties of cyanine dyes is their ability to form CJA, which results in much narrower absorption and emission peaks, along with a redshift in their spectra (in comparison to cyanine dye monomers). Cyanines are one of the few kinds of molecules whose absorbance and emission can be shifted in a broad spectral range from the ultraviolet to the near infrared (NIR),^[1] depending on the polymethine chain length and its terminal substituents.^[2]

This review surveys cyanines and their J-aggregates, with a focus on methods for their preparation and their characterization. Section 2 introduces cyanine dyes and their unique molecular properties. Section 3 summarizes the theoretical and experimental state of the art on CJA. Section 4 discusses the synthesis, characterization, and applications of CJA. Lastly, conclusions and points for future avenues of exploration are mentioned.

2. Introduction to Cyanine Dyes

Cyanine dyes have been known since the 1850s. Williams was probably the first chemist to produce a cyanine dye, when in 1856 he reacted crude quinoline with alkyl (ethyl, amyl) iodides, followed by treatment with silver oxide. This made a compound presenting "a blue of great beauty and intensity".^[3] In 1860, Williams named this dye 'cyanine' (from the Greek *kyanos* = blue).^[4] Through detailed investigations of the cyanine dye, in 1862, Hofmann found that it was composed of quinoline and lepidine (4-methylquinoline) derivatives, which came as no surprise, since the crude quinoline used by Williams contained a large amount of lepidine as an impurity.^[3-5]

In the following years, similar chromophores with a pronounced blue color were produced and cognates such as cryptocyanine, isocyanine, pseudoisocyanine, and pinacyanol were suggested.^[6] However, it was only decades later that the structures of these dyes, including Williams' cyanine, were reliably identified.^[7] At this point, it was realized that all these dyes have one feature in common; namely, that they consist of two heterocyclic units, which are connected by an odd number of methine groups (CH)_n (with $n = 1, 3, 5, \dots$). König introduced the term polymethine dyes in the 1920s, after work showing for the first time that the color of these dyes is mainly determined by the length of the polymethine chain.^[8]

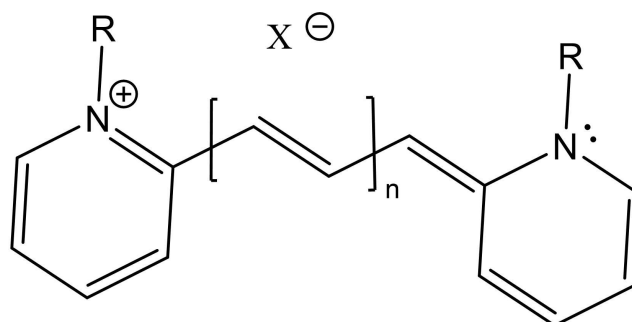


Figure 1. The general structure of cyanines ($n = 0, 1, 2, 3$).

[a] Dr. N. Dar, Dr. R. Ankari
Department of Physics, Faculty of Natural Science
Ariel University, Ariel 40700 (Israel)
E-mail: nitzanda@ariel.ac.il

© 2022 The Authors. Published by Wiley-VCH GmbH. This is an open access article under the terms of the Creative Commons Attribution Non-Commercial License, which permits use, distribution and reproduction in any medium, provided the original work is properly cited and is not used for commercial purposes.

The structure of cyanine dyes is dominated by aromatic heterocyclic donor (D) and acceptor (A) groups connected by polymethine chains of various lengths (Figure 1). The ideal polymethine electronic state is characterized by the alternation of the π -electron density on the polymethine chain and the formation of equal π -bond orders. The high oscillator strength of the dye in the polymethine state leads to the pronounced color. Cyanines can be cationic, anionic, or neutral (neutral cyanines are called merocyanines), but the alternating π -electron density distribution is independent of whether the molecule carries a charge or not.^[9] Thus, although the term polymethine dye is more accurate in terms of nomenclature, the term cyanine dye is widely used and will be used here interchangeably with the term polymethine.^[10]

2.1. Cyanine Structures and their Resulting Absorption Spectra

Cyanines are usually cationic molecules in which two terminal nitrogen heterocyclic subunits are linked by a polymethine bridge. Their names refer to the number of methine groups in the polyene chain (e.g., compounds with $n=0$ and $n=3$ are referred to as monomethine and heptamethine cyanine, respectively). The end sub-units, which contain a nitrogen atom, can be composed of two identical units or the units may be different from each other. The general structure of polymethine is shown in Figure 1.

The absorption range of the cyanine dyes is one of the largest for alternating single and double bond organic molecules, where each addition of a vinylene unit ($\text{CH}=\text{CH}$) causes a strong bathochromic shift to longer wavelengths of ~ 100 nm.^[11] Depending on the substituent, the absorption of pentamethine derivatives can reach the NIR region (> 750 nm), and heptamethine cyanines may show absorption even in the short-wave infrared (SWIR) regime (> 1000 nm), a unique property for these kind of molecules.^[12] Longer cyanines can also be prepared,^[13] but they are not commonly used because of their diminishing photostability, the broadening of their absorption spectrum^[14] and the fact that their absorption decreases when extending the polymethine chain length.^[15] However, the introduction of a cyclic rigid group in the polymethine chain can improve the stability of long-chain cyanine dyes.^[16]

To date, a large number of cyanine dyes has been synthesized and reviewed.^[17] In terms of their spectral properties, cyanine dyes have narrow absorption bands and extremely high extinction coefficients, often reaching $200,000 \text{ M}^{-1} \text{ cm}^{-1}$, leading to their pronounced color. Cyanine dyes are highly fluorescent in solution^[18] and their fluorescence efficiency massively increases upon binding the dyes with molecules that cause rigidification of the fluorophore.

2.2. Insights into the Polymethine Structure – Molecular Bonds, Electronic Structure and Spectral Transitions in Polymethines

A polymethine chain has an odd carbon atom and ionic conjugated π system. It is characterized by the alternation of the π -electron density along the chain and equal C–C bond orders that are close to 1.5.^[19] Hence, cyanines are nearly planar and very rigid. X-ray diffraction measurements on these dyes show that the most typical polymethine dye molecules are nearly planar in that they present less than a 15° angle between the planes of the heterocyclic rings,^[1a] therefore tending to aggregate.^[20]

The 1st excited singlet state (S_1) of cyanine dyes has an alternation of the charges on the carbon atoms in the methine groups. This charge alternates along the chromophore chain, and the charge inversion upon excitation helps to explain the high absorption of light and the relatively narrow electronic spectra. In contrast, polyenes, which are more commonly known, have an even number of carbon atoms and a neutral conjugated π system with an equal π -electron density on the carbon atoms of the methine groups. They exhibit lower absorption than their polymethine analogs, and, consequently, polymethines ground-state polarizability is at least three times larger than that of polyenes of similar size, which is crucial for the formation of molecular aggregates.^[20] There is a complete delocalization of π -electron density on the polymethine chain, whereas a π -conjugated system of polyenes exhibits characteristics mid-way between double bonds and single bonds. The planarity of cyanine molecules and their high electronic polarizability along the chain length is the basis for intermolecular interactions, leading to the phenomenon of J-aggregation (see Section 3).^[10,20]

A number of simplified models for the polymethine chain and the terminal atoms which neglect the molecule's substituents has been put forward, focussing on the bond length and bond orders of the ground (S_0) and excited (S_1) states. One prominent model that considers the possible transitions (localized $\pi \rightarrow \pi^*$, delocalized and terminal group transitions), the molecular structure in the excited state, and includes changes in bond length or angles (when excitation can be totally delocalized or partially localized) was published by Kachkovski and Tyutyulkov.^[6a,15,21] They suggested that the electronic transitions are an indication of the changes in the bond order, bond lengths and depend not only on the number of methine groups in the polymethine linear conjugated systems (molecular charge and nature of the terminal group), but also on the type of electronic transition. To conclude, the delocalized electronic structure of the polymethine chain is the basis of their high absorbance and planar arrangement.

2.3. Controlling the Spectral Properties of Cyanines

To develop novel applications for cyanine dyes, precise control of the electronic transitions is required, since it results in a specific change in the absorption or fluorescence spectrum of the molecule. The key rules characterizing the electronic

transitions in cyanines and their analogs are HOMO–LUMO orbital symmetry and large $S_0 \rightarrow S_1$ transition dipole moment. In other words, in cyanines, the longer the polymethine chain, the longer the absorption wavelength. Several possible methods have been described to control bathochromic shifts, which is a shift of the spectral band in the absorption and/or the emission spectrum of a molecule to a longer wavelength (also called redshift),^[22] in cyanine dyes. The addition of vinylene in a polar solvent induces a smaller bathochromic shift,^[16b] as well as a change in the structure of the terminal group,^[23] for example with electron-donating groups.^[23a] Polymethine cyclic groups on the chain may cause a bathochromic shift and can increase the quantum yield of the dyes, but this process is highly dependent on the nature of the cyanine and the precise experimental conditions.^[24] In addition, *solvatochromism*; that is, controlling the spectral shift of cyanine dyes by solvent replacement, might cause a bathochromic shift for cyanine dyes.^[25]

Thus, three main factors influence the preparation of NIR cyanine dyes and change the absorption and stability of cyanines: (1) Elongation of the methine chain, where the longer the methine chain, the larger the bathochromic shift; (2) Modification of the terminal groups; (3) Introduction of a cyclic ring/s inside the polymethine chain (Figure 2).^[2]

2.4. Introduction to Cyanine-like Molecules

A few well-known molecules exhibit chemical properties similar to cyanine. In some cases, they have better spectral performance than cyanine dyes. Due to the variety of their molecular structures, charges and reactivity, they could have different

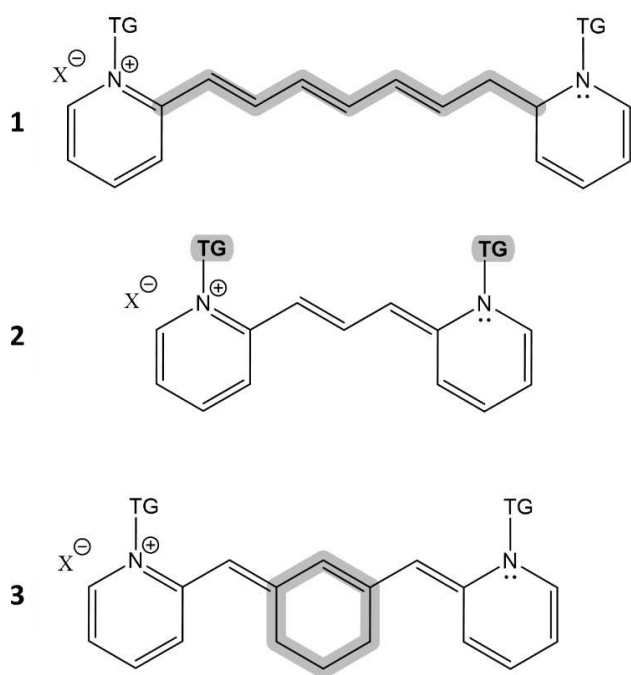


Figure 2. Three possible ways to prepare a stable highly fluorescent near IR cyanine dye. 1) Elongation of the methine chain. 2) Modifying the terminal groups (TG). 3) Introducing a ring within the polymethine chain.

possible applications such as for solar cells, nonlinear optics, batteries, bioimaging, photodynamic therapy and medical diagnostics.^[26]

The seven main types of cyanine-like molecules (Figure 3) are as follows:

- Hemicyanines:** In these molecules, one terminal is an amino group as part of a heterocycle, while the second terminal group is an open chain (see Figure 3a)
- Streptocyanines or ‘open-chain cyanines’:** In these molecules, the two terminals of the chromophore, the amino and imino groups, are open chains (Figure 3b).
- Squaraines or diketocyclobutanes:** These molecules, which have similar absorption to cyanines, are characterized by an aromatic four-membered ring system. Unlike cyanines, the counter ion is part of the molecule. Most squaraines are prone to a nucleophilic attack in the center of the four membered ring, which is highly electron deficient (Figure 3c).
- Croconates:** These molecules have a 5-membered aromatic ring and are used in solar cell research.^[27] In comparison to cyanines, they present a redshifted fluorescence spectrum, especially when sulfur or selenium replace the oxygen atoms bound to the ring (Figure 3d).
- Merocyanine dyes:** These dyes have an amino and a carbonyl group as end groups of the polyene structural element. Both a neutral and a zwitterionic resonance structure have been described for this compound. In merocyanine, there is a transition between polyene and polymethine (Figure 3e).^[28]
- Oxonol dyes:** Their terminal groups contain oxygen as a heteroatom and they are negatively charged, in contrast to cyanine that only contains nitrogen (Figure 3f).
- Flavylium-based polymethine:** This family of molecules has a side chain and a heterocycle that contains an oxonium ion. Recently, flavylium molecules have been found and successfully applied for SWIR imaging.^[29]

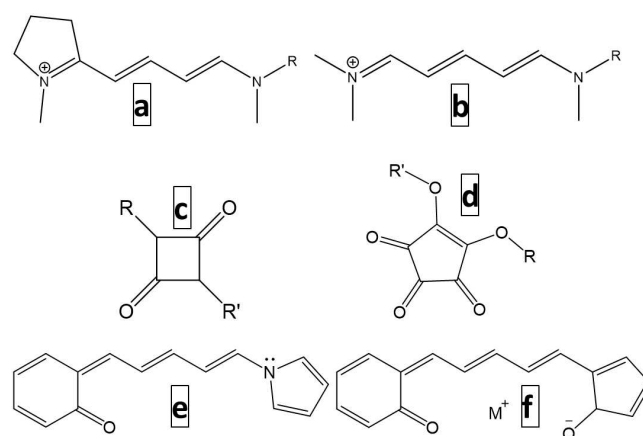


Figure 3. Structures examples of (a) hemicyanine, (b) streptocyanine, (c) squaraine, (d) croconate, (e) merocyanine and (f) oxonol dyes.

3. Concise Introduction to J-Aggregates

J-aggregates, which were discovered by Jelley and Scheibe,^[30] have an abnormally narrow, high-intensity, bathochromically shifted optical absorption band arising from the aggregation of polymethine dyes. The aggregation of cyanine monomers, which are part of the polymethine family, leads to the longer absorption wavelength, called the bathochromic shift. The J-aggregates are formed by a non-covalent polymer-like supramolecular structure that shows very narrow spectral bands. Several theories have been suggested to describe the structure of J-aggregates, but none have been shown to provide a comprehensive model for J-aggregate formation.^[31] This section reviews classical and more recent contemporary J-aggregate formation theories. As each theory refers to different aspects of CJA, they cannot be compared. This section followingly focusses on model for CJA, their advantages of and their methods of preparation.^[10,32]

3.1. The Frenkel Exciton Model

The Frenkel model for J-aggregation was proposed by Yacov Frenkel in 1931, soon after its discovery in 1926, to explain the nature of the spectral J-band.^[33] In this model, the specific structure of the dye has no influence, and the J-band is explained by the fast moving Frenkel exciton, which acts to average out the quasistatic disorders in the electronic transition energies of molecules in the linear J-aggregate.^[34] According to this theory, which was first exemplified with polymethine dyes,^[35] the Frenkel exciton is created by the excitation of an organic substance when the interaction between the hole and the electron is strong (~ 0.5 eV) such that the excited molecular state moves from one site to another.^[36] Conversely, the Wannier–Mott exciton model describes an exciton whose radius significantly exceeds the characteristic unit cell of a crystal lattice. Unlike the Frenkel excitons, the Wannier–Mott exciton is a moving electron-hole pair encompassing several molecules, and the exciton is weakly coupled (~ 0.01 eV), with a radius larger than that of the Frenkel exciton (an illustration of these two excitons appears in Figure 4).^[36b] Both exciton models are used to interpret experimental data related to crystals with

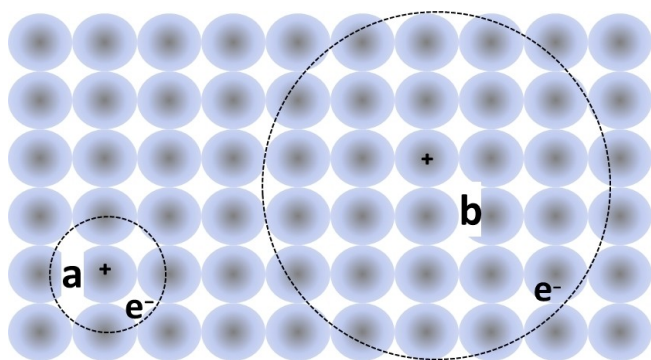


Figure 4. An illustration of (a) the Frenkel exciton and (b) the Wannier–Mott exciton.

different types of bonds. This is because Frenkel and Wannier–Mott excitons correspond to two limiting situations arising from electron-hole coupling, where in the former case the electron and the hole become tightly bound and localized on a single molecule. One should bear in mind that excitons are easily delocalized.^[32] In fact, J-aggregates have excellent capability to delocalized their exciton.^[10] Despite its simplicity, the Frenkel model has been shown to account not only for the shape of the J-band and the aggregates of different geometries, but also their nontrivial temperature, spectral dynamics^[37] and nonlinear response.^[38] This model has also been successfully applied to describe the optical and transport properties of conjugated polymers.^[39]

However, each theory suffers from several drawbacks. A quantitative interpretation of the small width and the entire shape of the J-band in the framework of the exciton theory was put forward by Knapp, Scherer, and Fischer.^[34,40] The problem of the optical band shape of monomers in polymethine dyes is still unresolved, resulting in the absence of a theoretical explanation for experimental data (e.g., as obtained by Brooker et al.^[41]).

A newer theory of intermolecular charge transfer views the J-band as an elementary charge which transfers along the J-aggregate's chromophore, dynamically pumped by the random reorganization of the nuclei in the nearby environment at a resonance between electronic and nuclear movements. In contrast to the Frenkel exciton theory, the structure of the polymethine dye does modify the J-bands.^[39b,42]

3.2. Kasha's Basic Theory of J-Aggregates and its Extension

Michael Kasha's theory dates back to 1965,^[43] and has been applied to associate the geometry of the aggregates to their photophysical properties.^[44] The theory, based on Frenkel exciton theory in which two-level chromophores are coupled via dipole-dipole interactions, is used to describe spectroscopic phenomena in molecular aggregates.^[43–44] Kasha showed that the Coulombic coupling between two molecules, as determined by the alignment of their transition dipoles, induces a redshift in the main absorption spectral peak, which are followed by a change in the radiative decay rate as compared to uncoupled molecules. In H-aggregates, the transition dipole moments that align "side-by-side" lead to a spectral blueshift and suppress the radiative decay rate, whereas in J-aggregates, the transition dipole moments align "head-to-tail" and lead to a spectral redshift and an enhanced radiative decay rate (Figure 5).

Kasha's theory was originally developed to explain the significant red-shifted absorption peaks in the molecular aggregates observed in cyanine dyes in solution. By modeling them as dimers or linear chains of molecules interacting through dipolar excitonic couplings, Kasha directly associated the angle between the transition dipoles and the chain axis with the monomer-aggregate absorption peak shift. Two main conclusions have been drawn from Kasha's model: (i) a red-shifted peak corresponds to a head-to-tail configuration, which gives rise to negative excitonic couplings in the dyes, resulting in J-aggregates, and (ii) a blueshifted peak corresponds to a

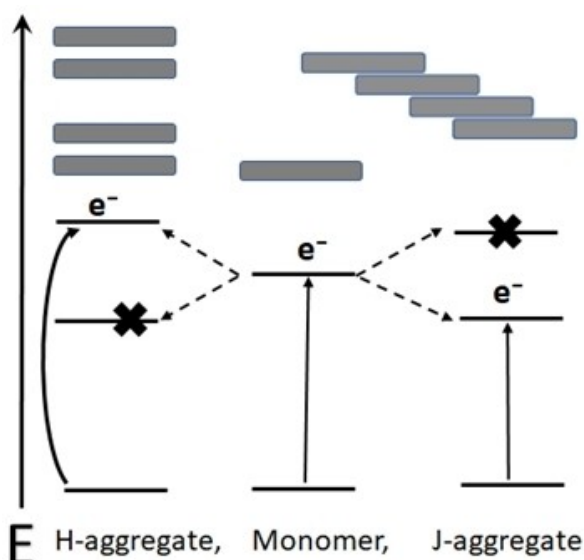


Figure 5. Energy levels and structure of a monomer and its H- and J-aggregates.

side-by-side configuration that leads to positive excitonic couplings, creating H-aggregates.^[43–45] A typical blueshifting in H-aggregates results from transitions to the lowest energy exciton state are not optically allowed, whereas transitions to the highest energy exciton state are enhanced due to the electronic coupling between molecules (Figure 5).^[46]

However, Kasha's theory fails to account for certain types of aggregates. For example, it cannot explain the vibronic fine structure or vibronic sidebands, including their polarization properties, since to do so, local exciton-vibrational coupling must be included.^[47] Hestand et al. extended Kasha's H and J-aggregates theory by incorporating vibronic coupling and intermolecular charge transfer, which led to a better understanding of the relationship between aggregate structure and photophysics.^[32] In 2019, Chuang et al. built on Kasha's theory to present a general framework for 1D and 2D systems for extracting key microscopic packing parameters. They used temperature-dependent linear spectroscopy and the direction of the absorption peak shift with increased temperature to successfully account for sucrose encapsulation.^[48] They generalized Kasha's model by incorporating the temperature dependent absorption peak shift, and the monomer-aggregate absorption peak shift that defines J- and H-aggregates. They showed that short-range interactions dominate when determining the direction of the temperature dependent peak shift, explaining the previously observed merocyanine blueshifted J-aggregates.^[49]

3.3. Why are Cyanine Dyes Better for CJA Formation?

Several aromatic compounds can form J-aggregates, including porphyrins,^[50] polyaromatic compounds,^[51] poly(3-hexylthiophene)^[52] and perylene bisimides.^[53] However, non-cyanine

molecular aggregates in solution are sparse and most of them only form at high concentrations or require special stabilizing conditions. In addition, the aggregation energy of cyanine dyes when creating CJA is high (0.5–1 eV) due to the high polarizability of these dyes.^[20] The other advantages of CJA are that the singlet excited state of the cyanine (S_1) bond order is 1.5, and its nearly linear conformation remains the same as the singlet ground state (S_0), leading to a high molar absorption coefficient^[20] and superradiance.^[54] Furthermore, the absorption and the fluorescence peaks of CJA are narrow. These properties, which are unique to CJA, make them the ultimate choice to prepare J-aggregates and their applications.^[10,20] Thus, a thoughtful design of the CJA structure can lead to a broad range of emitting dyes, from ultraviolet to the NIR regime.^[11]

3.4. How is CJA Formation Controlled?

A number of parameters cause reactions in the monomers, leading to J-aggregates in a simple way and with a high yield. Although there is no rigorous theory, a few 'rules of thumb' can be suggested to synthesize CJA with a large spectral shift and high stability.

Consistent with the law of entropy, the lower the temperature, the higher the probability to form CJA.^[17c,30a] In addition, from a thermodynamic point of view, the concentration of cyanine dyes is also an important factor, since higher concentrations ($> 10^{-3}$ M) are more likely to form CJA. In aqueous solutions, the pH of the solvent and the type of counter ion are also important. For example, CJA were prepared by the addition of NaCl to an aqueous solution.^[55] In addition, the longer the cyanine chain, the fewer its conformations and the easier the aggregation.^[2] A linear chain enhances dense packing aggregation due to the π - π interactions of the cyanine molecules, so that a linear polymethine chain requires an all-*trans* configuration.

Molecule size is also an important factor in their aggregation. On the one hand, large molecules convert to J-aggregate more easily, but on the other hand, a short methine chain makes it easier to obtain a J-aggregate. Thus, more work is needed to better understand the parameters that promote or inhibit aggregation. Stabilizing terminal groups can also enhance the formation of CJA, but it has been shown that only specific groups enhance aggregation (although there has yet to be a clear explanation).^[56] Another way to facilitate aggregation is by adding surfactants, such as sulfates, which can enhance the formation of CJA.^[20] Lengthening the polymethine chain by the introduction of new vinylene groups induces a substantial bathochromic shift of the absorption peaks, as does the addition of heterocyclic systems (used as terminal groups with a large effective length), modification of the open polymethine chain, branching of the polymethine chain, introducing donor or/and acceptor substituents in both the chain and terminal residues, etc.^[2] The concentration of the cyanine dyes, the type of solvent, the pH (for aqueous solutions), the temperature adjustment and the type of the counter ion all influence the aggregation of a cyanine dye.^[2,20] Although there is no

comprehensive theory that explains how to prepare J-aggregates from cyanine dyes and similar molecules, the above findings provide important information on the experimental conditions that should be taken into consideration when attempting to produce specific CJA. Figure 6 presents a chart of the parameters that influence the formation of CJA.

4. Synthetic Methods for CJA and Characterization

4.1. Overview of the Most Recent Synthesis Methods for CJA

The synthesis of cyanine dyes is usually enabled by a condensation reaction between terminal groups, which includes nitrogen, and the polymethine chain. If the goal is to put a substituent on the methine chain, an additional step is required, as discussed in the next section. Other methods for preparation of CJA, such as self-assembly,^[17a-c,f,57] preparation on a supporting scaffold^[17d,58] or on a plasmonic metallic nanostructure^[59] are beyond the scope of this review.

Wei Cao et al. synthesized CJA in a fluorosolvent (organofluorine compounds used as the major solvent).^[47] They prepared a fluoro-substituted cyanine, characterized the aggregates by AFM, and measured the fluorescence emission in different solvents. They found high solvatochromism of different organic solvents, including a fluorosolvent. The quantum yield reached 6.9% and absorbance coefficient (ϵ) was 153,000. They also showed that there are fluorosolvent substitutes of CJA which were dissolved in non-aqueous media. However, this study had a number of weaknesses, including a complicated multi-step synthesis procedure for the cyanine dye, the fact that neither TEM nor SEM was conducted, and as far as NIR bioimaging is concerned, the fluorescence emission peak of the J-aggregates was located in the visible region (~ 600 nm). Since in this regime of the electromagnetic spectrum many alternative commercial, cheap dyes with high fluorescence and good photostability are available, the complicated synthesis procedure does not seem warranted although it paves the way

for similar products when using dyes with longer wavelength emissions.

Caixia Sun et al. synthesized two kinds of cyanine molecules and turned them into J-aggregates with an absorbance peak at 1360 nm.^[60] The aggregates were characterized by TEM and DLS. The team found that their J-aggregates were photostable and presented thermostability at temperatures up to 100 °C. The biocompatibility was demonstrated through low aggregate cytotoxicity and aggregate stability in brine, in phosphate buffer saline (PBS) and in blood solutions, thus enabling the use of CJA for vascular bioimaging in rats. Nevertheless, despite the high redshift and good biocompatibility, the absorbance was moderate, $\epsilon \approx 50,000$, and the quantum efficiency was very low ($\Phi \approx 0.05\%$). In addition, the preparation of this cyanine dye requires a multi-step synthesis which is complicated and time-consuming.

CJA in hollow silica fibers were fabricated by Chen Wei et al.^[61] The heptamethine cyanine dyes resulted in an absorption peaking the NIR region, between 920–1060 nm, and a fluorescence emission spectrum at 1000–1700 nm. The aggregates, which were encapsulated in PEG, were found to be biocompatible and stable in PBS. Cytotoxicity studies of the ensemble were followed by in vivo imaging of mice. However, although the absorption coefficient of the aggregates was high at $\epsilon = 390,000$, the quantum yield for the cyanine aggregates was very low ($\Phi = 0.012\%$). The fabrication procedure of the aggregate involved numerous steps, which makes the preparation time-consuming. The aggregates were characterized by low-resolution TEM (100 nm), so that little information could be obtained to define their structure. The photostability of the aggregates was better than that of the cyanine monomers; however, it was measured for only 2 hours after the initial irradiation, so it remains unclear whether it is stable under other conditions.

Double-walled CJA absorption before and after mild oxidation was measured by Eisele et al.^[31a] Cyanine dyes were aggregated in a mixture of water and methanol. They formed a double-wall structure which was characterized by CryoTEM. The monomeric cyanines presented an absorption peak at 530 nm, while the CJA absorbed at a wavelength of 590 nm. The CJA changed their spectra after oxidation by silver ions, showing that apart from the absorption peak at 600 nm, all the other peaks decreased. The team concluded that the outer wall and the inner wall of the CJA have different spectra, where the outer wall is more permeable to oxidation by silver ions than the inner wall. As noted above, CJA should be very fluorescent, but no fluorescence spectra were shown. In addition, no explanation on why the walled structure had formed was given.

In a study by Shanker et al.,^[62] the formation of CJA with the same structure but with different polymethine lengths was carried out through counter ion exchange. The cyanines were ensembled into a silica nanofiber. Thiocarbocyanine iodide was reacted with silver acetate to make thiocarbocyanine acetate because the latter compound is more water-soluble, and both the H and J-aggregates of cyanine were formed. Investigation of the crystalline phases on the silica fiber was conducted by SEM and TEM, and the presence of cyanine crystals was shown

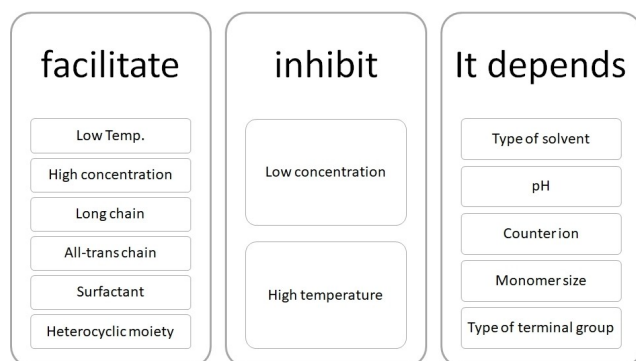


Figure 6. Parameters that facilitate and/or inhibit the formation of cyanine J-aggregates.

by XRD. NMR analyses were also carried out to determine the cyanine structure after the anion exchange reaction with the acetate. The absorption spectra were measured with maxima between 500–650 nm depending on the dye and the exact experimental conditions. Fluorescence spectra were reported, but no quantum yield and no further data have been included. Finally, no applications of the aggregate were described.

These articles thus demonstrate the formation of CJA with high absorbance and the ample structures of CJA. However, each study suffers from weaknesses including low quantum yield, short emission wavelengths, low photostability, incompatibility for biological usages, poor characterization, and tedious preparation procedures.

Two easier methods for the preparation of CJA are presented below:

1. **Micelles:** Generally, in micelles, soluble cyanine dyes sparingly reinsert into a capsule surrounded by an amphiphilic surfactant (featuring both hydrophilic head groups and hydrophobic alkyl chains), thus leading to the solubilization of cyanine molecules in, for example, phospholipid-polyethylene glycol (PEG). An example of micellar encapsulation was recently reported by Cosco et al.,^[29] for use in NIR and SWIR bioimaging. Micelle encapsulation has several advantages: it can enhance the aggregation of the cyanine dye, it can inhibit the degradation of cyanine dye by processes such as photobleaching, and, with a suitable surfactant, can make the CJA biocompatible, thus extending the bioimaging applications of CJA.^[61]
2. **The Langmuir–Blodgett (LB) technique,** which creates a monolayer of aggregates between an aqueous and an organic phase, followed by pulling out the material onto a surface (see Figure 7). The LB technique is a powerful tool that makes it possible to assemble organic molecules, which are typically amphiphilic, into two-dimensional molecular sheets.^[63] As shown in Figure 7, amphiphilic molecules are spread on the water's surface using a volatile solvent such as chloroform, benzene, or toluene. After the volatile solvent is evaporated, the molecules on the water surface are compressed using a barrier. The monomolecular film at the air/water interface is often referred to as the Langmuir film. Two well-known methods have been developed to transfer the Langmuir film onto solid substrates: (1) The vertical dipping of the substrate into the film, the LB technique (Figure 7a); (2) The horizontal lifting technique, which is called the Langmuir–Schaefer technique, as shown in Figure 7b. Sometimes both the vertical dipping and the horizontal lifting methods are categorized as the LB method. There has been a tremendous number of modifications and upgrades of both the LB and Langmuir–Schaefer techniques.^[63–64]

4.2. Analytical Methods for CJA Characterization

The characterization of cyanines includes structural analyses with NMR and CD spectroscopy, and morphological analyses, such as SEM, XRD and cryoTEM. For a simple and crucial one-step characterization of CJA, the easiest analytical method is

fluorescence spectroscopy, tracing the CJA peak's position relative to the monomer. One can also calculate the quantum yield the fluorescence lifetime^[65] and the photostability of the CJA.^[66]

However, solutions of CJA may exhibit low fluorescence quantum yields compared to the monomer due to non-radiative decay.^[67] In those cases, interpretation of the fluorescence spectra is quite challenging. Therefore, absorbance spectroscopy, which provides the H/J aggregate-to-monomer ratio to determine the level of efficiency of the absorbance, and which also serves to assess the purity of the sample by observing smaller peaks, is important.

CryoSEM and CryoTEM are essential for categorizing CJA because Cryo techniques freeze the solution immediately so that the structure and morphology of the aggregate can be observed similar to the solution state at which the CJA were formed and investigated. Berlepsch et al. investigated the microstructure of dye aggregates by CryoTEM.^[68] This technique provides direct high-resolution images of the aggregates in their native environment that are free of the drying artifacts related to the specific sample preparation technique. Although this technique does not generally resolve the aggregates' internal molecular organization, it often yields valuable quantitative information on the nanometer scale that can be used to improve theoretical structure models.^[69] One disadvantage of cryo-TEM has to do with specimen preparation, which can be tedious and time-consuming. To enhance the low contrast, heavy metal compounds can be introduced as well as staining additives which also enhance the contrast by electron scatter-

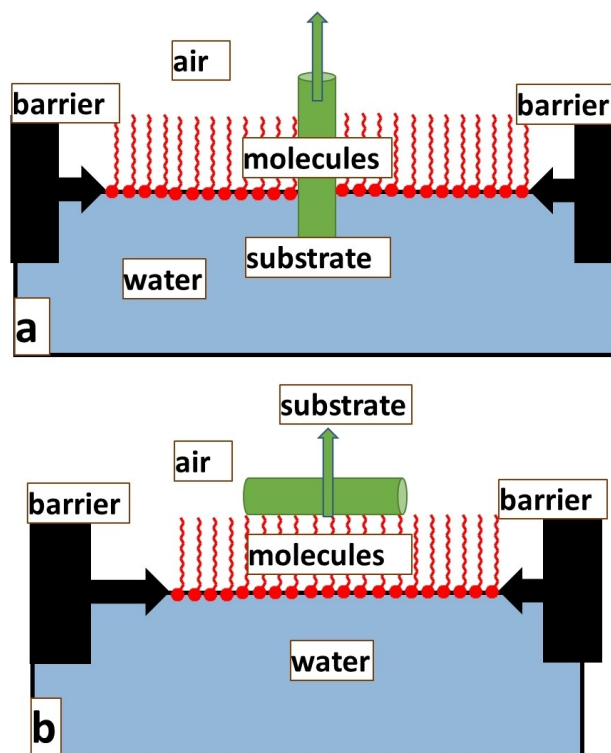


Figure 7. The Langmuir–Blodgett technique (a) with the vertical lift of the substrate and (b) with a horizontal lift of the substrate.

ing absorption effects. In addition, TEM artifacts can also appear, so a skilled technician is required to interpret the images.

Other methods for CJA characterization include NMR spectroscopy and X-ray diffraction (XRD) analysis. To determine the crystalline structure of the CJA, 1D and 2D NMR spectroscopy can be used. ^1H - and ^{13}C -NMR spectroscopy are commonly used for characterization of new cyanine syntheses.^[62,70] The phase of the crystalline CJA can also be observed by NMR and XRD as well as the liquid crystal structure of the CJA.^[70] Recently, multidimensional NMR methods such as diffusion ordered spectroscopy (DOSY) have been utilized to characterize CJA in their solution state.^[71] NMR spectroscopy serves to identify the molecular structure in solution as well as the aggregation parameters. X-ray crystallography yields information on the aggregation state of the cyanine when it crystallizes sufficiently. However, in contrast to NMR spectroscopy, the CJA must be crystallized before they can be observed.

A less common method, but one that can be implemented to analyze CJA, is circular dichroism (CD) spectroscopy, which is used to determine the optical isomerism and secondary structure of the CJA. Slavnova et al. added chiral molecules to CJA to explore the CD spectrum.^[72] Indirect methods such as dynamic light scattering (DLS) can help characterize the size, shape and aggregation number of supramolecular dye assemblies.^[73] Atomic force microscopy is used to examine the surface of the CJA or if they are built in another substrate.^[74] Infrared (IR) spectroscopy shows the intermolecular interactions between the individual cyanines in the CJA.^[75] More detailed information on the characterization of CJA can be found in References [74,76].

4.3. CJA Applications

Due to their unique spectroscopic properties, CJA have numerous applications. For example, before the advent of digital cameras, cyanines were widely used for photo development.^[77] Today, CJA are used in solar cells, as a photovoltaic layer, due to their high absorption coefficient (ϵ) and high electron transmittance^[78] and in light harvesting.^[79] CJA also play an important role as chemical sensors^[80] and shortwave infrared emitters,^[81] and are widely used in biomedical applications, providing bright, biosafe organic chemicals for in vivo imaging.^[29,60,81] In comparison to quantum dots, which are also widely used for NIR and SWIR bioimaging,^[82] CJA present a safer option for in vivo imaging. Many quantum dots have high toxicity and their excretion from the body is also a drawback. Carbon nanotubes,^[83] which are also widely used for NIR in vivo imaging, suffer from low quantum yields^[84] and difficulties controlling their size distribution, which results in a broad absorption peak and low fluorescence.^[83,85] Lanthanides are also intensively used in bioimaging,^[82,86] since they present a narrow emission band and high photostability, but very few lanthanides have both an emission of about 1100 nm and high quantum yield.^[82] For these reasons, CJA are a real bioimaging

alternative to quantum dots, lanthanides and carbon nanotubes.

5. Conclusion

This review discussed cyanine dyes and their J-aggregates. It summarized theories on cyanine J-aggregates (CJA), suggested strategies for their synthesis, and methods for their characterization, based on state-of-the-art publications. Attention was drawn to the factors that impede the use of suitable cyanine dyes and their aggregates, such as synthetic difficulties, stability and quantum efficiency for a specific, targeted application. Despite the current difficulties, new frontiers in research have made huge advances in both the fundamental understanding and applicative use of CJA in solar cells and bioimaging. Thus, cyanine dyes and their aggregates are likely to have a bright future.

Acknowledgements

The work was supported by the council for higher education, Israel.

Conflict of Interest

The authors declare no conflict of interest.

Data Availability Statement

Data sharing is not applicable to this article as no new data were created or analyzed in this study.

Keywords: CryoEM · cyanines · J-aggregates · polymethines · UV/Vis spectroscopy

- [1] a) T. H. James, *New York: Macmillan*, The Theory of the Photographic Process, **1966**; b) T. Tani, *Photographic sensitivity: theory and mechanisms*, Oxford University Press on Demand, **1995**.
- [2] J. L. Bricks, A. D. Kachkovskii, Y. L. Slominskii, A. O. Gerasov, S. V. Popov, *Dyes Pigm.* **2015**, *121*, 238–255.
- [3] C. G. Williams, *Earth Environ. Sci. Trans. R. Soc. Edinburgh* **1857**, *21*, 377–401.
- [4] W. Spalteholz, *Ber. Dtsch. Chem. Ges.* **1883**, *16*, 1847–1852.
- [5] A. W. V. Hofmann, *Proc. R. Soc. London* **1863**, 410–418.
- [6] a) N. Tyutyulkov, J. Fabian, A. Mehlhorn, F. Dietz, A. Tadjer, *Polymethine dyes*, St. Kliment Ohridski University Press, Sofia, **1991**, 111–164; b) R. M. Christie, *Colour Chemistry*, Royal Society of Chemistry, London, **2001**, 104; c) H. Zollinger, *Color chemistry: syntheses, properties, and applications of organic dyes and pigments*, VHC, Zurich, **2003**.
- [7] a) W. König, *J. Prakt. Chem.* **1906**, *73*, 100–108; b) W. König, O. Treichel, *J. Prakt. Chem.* **1921**, *102*, 63–84.
- [8] W. König, *J. Prakt. Chem.* **1926**, *112*, 1–36.
- [9] S. Dähne, D. Leupold, *Angew. Chem. Int. Ed. Engl.* **1966**, *5*, 984–993.
- [10] F. Würthner, T. E. Kaiser, C. R. Saha-Möller, *Angew. Chem. Int. Ed.* **2011**, *50*, 3376–3410; *Angew. Chem.* **2011**, *123*, 3436–3473.

- [11] a) A. Mishra, R. K. Behera, P. K. Behera, B. K. Mishra, G. B. Behera, *Chem. Rev.* **2000**, *100*, 1973–2012; b) H. Kuhn, *J. Chem. Phys.* **1949**, *17*, 1198–1212.
- [12] R. P. Haugland, *Handbook of fluorescent probes and research products*, Molecular probes, Inc, PO Box 22010 Eugene, OR 97402-0414, USA, or 15 rue des Champs, 92600 Asnieres, Paris, **1992**.
- [13] H. Shindy, M. El-Maghraby, M. Goma, N. Harb, *Chem. Int.* **2020**, *4*, 187–199.
- [14] J. H. Lim, O. V. Przhonska, S. Khodja, S. Yang, T. Ross, D. J. Hagan, E. W. Van Stryland, M. V. Bondar, Y. L. Slominsky, *Chem. Phys.* **1999**, *245*, 79–97.
- [15] A. Kachkovski, O. Zhukova, *Dyes Pigm.* **2004**, *63*, 323–332.
- [16] a) N. Monich, Z. A. Krasnaya, I. Levkoev, V. Kucherov, *Chem. Heterocycl. Compd.* **1981**, *17*, 1192–1197; b) J. Fabian, H. Nakazumi, M. Matsuoka, *Chem. Rev.* **1992**, *92*, 1197–1226.
- [17] a) B. Shapiro, L. Sokolova, V. Kuz'min, A. Tolmachev, Y. L. Slominskii, Y. L. Briks, *Nanotechnol. Russ.* **2012**, *7*, 205–212; b) B. J. Walker, A. Dorn, V. Bulovic, M. G. Bawendi, *Nano Lett.* **2011**, *11*, 2655–2659; c) R. Passier, J. P. Ritchie, C. Toro, C. Diaz, A. E. Masunov, K. D. Belfield, F. E. Hernandez, *J. Chem. Phys.* **2010**, *133*, 134508; d) M. Liu, A. Kira, *Thin Solid Films* **2000**, *359*, 104–107; e) H. Von Berlepsch, S. Kirstein, C. Böttcher, *Langmuir* **2002**, *18*, 7699–7705; f) A. K. Chibisov, T. D. Slavnova, H. Görner, *Chem. Phys. Lett.* **2010**, *498*, 63–66.
- [18] L. Mikelsons, C. Carra, M. Shaw, C. Schweitzer, J. Sciaiano, *Photochem. Photobiol. Sci.* **2005**, *4*, 798–802.
- [19] B. I. Shapiro, *Russ. Chem. Rev.* **2006**, *75*, 433.
- [20] J. L. Bricks, Y. L. Slominskii, I. D. Panas, A. P. Demchenko, *Methods Appl. Fluoresc.* **2017**, *6*, 012001.
- [21] A. D. Kachkovskii, *Russ. Chem. Rev.* **1997**, *66*, 647.
- [22] J. W. Verhoeven, *Pure Appl. Chem.* **1996**, *68*, 2223–2286.
- [23] a) I. Davidenko, J. Slominsky, A. Kachkovskii, A. Tolmachev, *Ukr. J. Chem.* **2008**, *74*, 105–113; b) D. Krotko, K. Fedotov, A. Kachkovskii, A. Tolmachev, *Dyes Pigm.* **2005**, *64*, 79–84; c) A. E. Asato, D. T. Watanabe, R. S. Liu, *Org. Lett.* **2000**, *2*, 2559–2562; d) R. S. Liu, A. E. Asato, *J. Photochem. Photobiol. C* **2003**, *4*, 179–194.
- [24] S. Webster, L. A. Padilha, H. Hu, O. V. Przhonska, D. J. Hagan, E. W. Van Stryland, M. V. Bondar, I. G. Davydenko, Y. L. Slominsky, A. D. Kachkovskii, *J. Lumin.* **2008**, *128*, 1927–1936.
- [25] a) H. Shindy, *Dyes Pigm.* **2017**, *145*, 505–513; b) A. Yu, C. A. Tolbert, D. A. Farrow, D. M. Jonas, *J. Phys. Chem. A* **2002**, *106*, 9407–9419.
- [26] a) A. V. Kulinich, A. A. Ishchenko, *Russ. Chem. Rev.* **2009**, *78*, 141; b) H. Moustroph, *Phys. Sci. Rev.* **2022**, *7(1)*, 37–43; c) K. Iliina, W. M. MacCuaig, M. Laramie, J. N. Jeouty, L. R. McNally, M. Henary, *Bioconjugate Chem.* **2019**, *31*, 194–213.
- [27] R. K. Chitumalla, M. Lim, X. Gao, J. Jang, *J. Mol. Model.* **2015**, *21*, 297.
- [28] W. Rettig, M. Dekhtyar, *Chem. Phys.* **2003**, *293*, 75–90.
- [29] E. D. Cosco, A. L. Spearman, S. Ramakrishnan, J. G. Lingg, M. Saccomano, M. Pengshung, B. A. Arús, K. C. Wong, S. Glasl, V. Ntziachristos, *Nat. Chem.* **2020**, *12*, 1123–1130.
- [30] a) G. Scheibe, *Angew. Chem.* **1937**, *50*, 212–219; b) E. Jelley, *Nature* **1937**, *139*, 378.
- [31] a) D. M. Eisele, C. Cone, E. A. Bloemsmas, S. Vlaming, C. Van Der Kwaak, R. J. Silbey, M. G. Bawendi, J. Knoester, J. P. Rabe, D. V. Bout, *Nat. Chem.* **2012**, *4*, 655–662; b) F. C. Spano, C. Silva, *Annu. Rev. Phys. Chem.* **2014**, *65*, 477–500.
- [32] N. J. Hestand, F. C. Spano, *Chem. Rev.* **2018**, *118*, 7069–7163.
- [33] J. Frenkel, *Phys. Rev.* **1931**, *37*, 1276.
- [34] E. Knapp, *Chem. Phys.* **1984**, *85*, 73–82.
- [35] S. P. McGlynn, T. Azumi, M. Kinoshita, *Molecular spectroscopy of the triplet state*, Prentice Hall, Englewood Cliffs, NJ, **1969**.
- [36] a) V. Agranovich, *Theory of Excitons*, Nauka, Moscow, **1968**; b) M. Knupfer, *Appl. Phys. A* **2003**, *77*, 623–626.
- [37] a) D. Heijs, V. Malyshev, J. Knoester, *Phys. Rev. Lett.* **2005**, *95*, 177402; b) D. Heijs, V. Malyshev, J. Knoester, *J. Lumin.* **2006**, *119*, 271–276.
- [38] J. R. Durrant, J. Knoester, D. A. Wiersma, *Chem. Phys. Lett.* **1994**, *222*, 450–456.
- [39] a) V. V. Egorov, M. V. Alfimov, *Phys. Usp.* **2007**, *50*, 985; b) V. V. Egorov, *Phys. Procedia* **2009**, *2*, 223–326.
- [40] a) E. Knapp, P. Scherer, S. Fischer, *Chem. Phys. Lett.* **1984**, *111*, 481–486; b) G. D. Scholes, G. Rumbles, *Annu. Rev. Nano Res.* **2008**, *103*–157; c) M. Pope, C. E. Swenberg, *Electronic processes in organic crystals and polymers*, Vol. 56, Oxford University Press on Demand, **1999**.
- [41] L. Brooker, R. Sprague, C. Smyth, G. Lewis, *J. Am. Chem. Soc.* **1940**, *62*, 1116–1125.
- [42] V. V. Egorov, *Chem. Phys.* **2001**, *269*, 251–283.
- [43] M. Kasha, H. R. Rawls, M. A. El-Bayoumi, *Pure Appl. Chem.* **1965**, *11*, 371–392.
- [44] M. Kasha, *Radiat. Res.* **1963**, *20*, 55–70.
- [45] U. Rösch, S. Yao, R. Wortmann, F. Würthner, *Angew. Chem. Int. Ed.* **2006**, *45*, 7026–7030; *Angew. Chem.* **2006**, *118*, 7184–7188.
- [46] F. C. Spano, *Acc. Chem. Res.* **2010**, *43*, 429–439.
- [47] W. Cao, E. M. Sletten, *J. Am. Chem. Soc.* **2018**, *140*, 2727–2730.
- [48] C. Chuang, D. I. Bennett, J. R. Caram, A. Aspuru-Guzik, M. G. Bawendi, J. Cao, *Chem* **2019**, *5*, 3135–3150.
- [49] A. Yamaguchi, N. Kometani, Y. Yonezawa, *Thin Solid Films* **2006**, *513*, 125–135.
- [50] a) D. C. Barber, R. A. Freitag-Beeston, D. G. Whitten, *J. Phys. Chem.* **1991**, *95*, 4074–4086; b) N. Micali, V. Villari, M. A. Castriciano, A. Romeo, L. Monsù Scolaro, *J. Phys. Chem. B* **2006**, *110*, 8289–8295; c) A. Koti, N. Periasamy, *Chem. Mater.* **2003**, *15*, 369–371; d) J. M. Chan, J. R. Tischler, S. E. Kooi, V. Bulovic, T. M. Swager, *J. Am. Chem. Soc.* **2009**, *131*, 5659–5666.
- [51] a) Y. Deng, W. Yuan, Z. Jia, G. Liu, *J. Phys. Chem. B* **2014**, *118*, 14536–14545; b) J. Xue, Q. Liang, R. Wang, J. Hou, W. Li, Q. Peng, Z. Shuai, J. Qiao, *Adv. Mater.* **2019**, *31*, 1808242.
- [52] E. T. Niles, J. D. Roehling, H. Yamagata, A. J. Wise, F. C. Spano, A. J. Moulé, J. K. Grey, *J. Phys. Chem. Lett.* **2012**, *3*, 259–263.
- [53] a) S. Herbst, B. Soberats, P. Leowanawat, M. Lehmann, F. Würthner, *Angew. Chem. Int. Ed.* **2017**, *56*, 2162–2165; *Angew. Chem.* **2017**, *129*, 2194–2197; b) W. Wagner, M. Wehner, V. Stepanenko, S. Ogi, F. Würthner, *Angew. Chem.* **2017**, *56*, 16008–16012; c) M. Hecht, F. Würthner, *Acc. Chem. Res.* **2020**, *54*, 642–653.
- [54] S. Özçelik, D. L. Akins, *J. Phys. Chem. B* **1999**, *103*, 8926–8929.
- [55] J. Xiang, X. Yang, C. Chen, Y. Tang, W. Yan, G. Xu, *J. Colloid Interface Sci.* **2003**, *258*, 198–205.
- [56] a) V. Tkachev, A. Tolmachev, Y. L. Slominskii, L. Chernigov, A. Babichenko, A. Smirnova, I. Krainov, *Ukr. Chem. J.* **1994**, *60*, 34–39; b) A. Tolmachev, Y. L. Slominskii, A. Ishchenko, in *Near-infrared dyes for high technology applications* (Eds. S. Daehne, U. Resch-Genger, O. S. Wolfbeis), Springer, **1998**, pp. 385–415.
- [57] a) B. Shapiro, E. Belonozhkina, V. Kuz'min, *Nanotechnol. Russ.* **2009**, *4*, 38–44; b) H. v. Berlepsch, C. Böttcher, *J. Photochem. Photobiol. A* **2010**, *214*, 16–21.
- [58] a) D. G. Whitten, K. E. Achyuthan, G. P. Lopez, O.-K. Kim, *Pure Appl. Chem.* **2006**, *78*, 2313–2323; b) O.-K. Kim, J. Je, G. Jernigan, L. Buckley, D. Whitten, *J. Am. Chem. Soc.* **2006**, *128*, 510–516.
- [59] a) I.-S. Lim, F. Goroleski, D. Mott, N. Kariuki, W. Ip, J. Luo, C.-J. Zhong, *J. Phys. Chem. B* **2006**, *110*, 6673–6682; b) A. M. Kelley, *Nano Lett.* **2007**, *7*, 3235–3240; c) A. Yoshida, N. Kometani, *J. Phys. Chem. C* **2010**, *114*, 2867–2872; d) G. Zengin, G. Johansson, P. Johansson, T. J. Antosiewicz, M. Käll, T. Shegai, *Sci. Rep.* **2013**, *3*, 3074; e) D. Melnikau, D. Savateeva, A. Susha, A. L. Rogach, Y. P. Rakovich, *Nanoscale Res. Lett.* **2013**, *8*, 134; f) S. Balci, *Opt. Lett.* **2013**, *38*, 4498–4501; g) Y. B. Zheng, B. K. Juluri, L. Lin Jensen, D. Ahmed, M. Lu, L. Jensen, T. J. Huang, *Adv. Mater.* **2010**, *22*, 3603–3607.
- [60] C. Sun, B. Li, M. Zhao, S. Wang, Z. Lei, L. Lu, H. Zhang, L. Feng, C. Dou, D. Yin, *J. Am. Chem. Soc.* **2019**, *141*, 19221–19225.
- [61] W. Chen, C.-A. Cheng, E. D. Cosco, S. Ramakrishnan, J. G. Lingg, O. T. Bruns, J. I. Zink, E. M. Sletten, *J. Am. Chem. Soc.* **2019**, *141*, 12475–12480.
- [62] G. Shanker, G. Hegde, C. Rodriguez-Abreu, *Liq. Cryst.* **2016**, *43*, 473–483.
- [63] Y. F. Miura, K. Ikegami, in *J-Aggregates: Volume 2* (Ed. T. Kobayashi), World Scientific, **2012**, pp. 443–514.
- [64] a) K. B. Blodgett, *J. Am. Chem. Soc.* **1935**, *57*, 1007–1022; b) G. L. Gaines, *Insoluble Monolayers at Liquid-Gas Interfaces*, Wiley, New York, **1966**.
- [65] M. Y. Berezin, S. Achilefu, *Chem. Rev.* **2010**, *110*, 2641–2684.
- [66] I. Martinić, S. V. Eliseeva, S. Petoud, *J. Lumin.* **2017**, *189*, 19–43.
- [67] J. S. Huff, P. H. Davis, A. Christy, D. L. Kellis, N. Kandada, Z. S. Toa, G. D. Scholes, B. Yurke, W. B. Knowlton, R. D. Pensack, *J. Phys. Chem. Lett.* **2019**, *10*, 2386–2392.
- [68] H. von Berlepsch, C. Böttcher, A. Ouart, C. Burger, S. Dähne, S. Kirstein, *J. Phys. Chem. B* **2000**, *104*, 5255–5262.
- [69] a) S. Ganapathy, G. T. Oostergetel, P. K. Wawrzyniak, M. Reus, A. G. M. Chew, F. Buda, E. J. Boekema, D. A. Bryant, A. R. Holzwarth, H. J. De Groot, *Proc. Nat. Acad. Sci.* **2009**, *106*, 8525–8530; b) S. Vlaming, R. Augulis, M. Stuart, J. Knoester, P. Van Loosdrecht, *J. Phys. Chem. B* **2009**, *113*, 2273–2283; c) J. Sperling, A. Nemeth, J. r Hauer, D. Abramavicius, S. Mukamel, H. F. Kauffmann, F. Milota, *J. Phys. Chem. A* **2010**, *114*, 8179–8189.
- [70] W. J. Harrison, D. L. Mateer, G. J. Tiddy, *J. Phys. Chem.* **1996**, *100*, 2310–2321.

- [71] a) A. Deshmukh, A. Bailey, L. Forte, X. Shen, N. Geue, E. Sletten, J. Caram, **2020**, ChemRxiv preprint DOI: 10.26434/chemrxiv.12609398.v1; b) C.-A. Shen, F. Würthner, *Chem. Commun.* **2020**, *56*, 9878–9881.
- [72] T. D. Slavnova, H. Görner, A. K. Chibisov, *J. Phys. Chem. B* **2011**, *115*, 3379–3384.
- [73] a) P. J. Collings, E. J. Gibbs, T. E. Starr, O. Vafek, C. Yee, L. A. Pomerance, R. F. Pasternack, *J. Phys. Chem. B* **1999**, *103*, 8474–8481; b) B. Neumann, K. Huber, P. Pollmann, *Phys. Chem. Chem. Phys.* **2000**, *2*, 3687–3695.
- [74] H. Yao, in *J-aggregates: Volume 2*, World Scientific, **2012**, pp. 403–441.
- [75] T. Kobayashi, J. Du, Y. Kida, in *J-aggregates: Volume 2* (Ed. T. Kobayashi), World Scientific, **2012**, pp. 1–47.
- [76] H. von Berlepsch, C. Böttcher, in *J-aggregates: Volume 2* (Ed. T. Kobayashi), World Scientific, **2012**, pp. 119–153.
- [77] a) H. Saijo, M. Shiojiri, *Microsc. Res. Tech.* **1998**, *42*, 123–138; b) B. Shapiro, L. Rozhkova, Y. L. Slominskii, A. Tolmachev, *High Energy Chem.* **2004**, *38*, 330–332; c) S. Watanabe, T. Tani, *J. Imaging Sci. Technol.* **1995**, *39*, 81–85.
- [78] R. Hany, B. Fan, F. A. de Castro, J. Heier, W. Kylberg, F. Nüesch, *Prog. Photovoltaics* **2011**, *19*, 851–857.
- [79] É. Boulais, N. P. Sawaya, R. Veneziano, A. Andreoni, J. L. Banal, T. Kondo, S. Mandal, S. Lin, G. S. Schlau-Cohen, N. W. Woodbury, *Nat. Mater.* **2018**, *17*, 159–166.
- [80] a) N. H. Mudliar, P. M. Dongre, P. K. Singh, *Sens. Actuators B* **2019**, *301*, 127089; b) T.-I. Kim, B. Hwang, B. Lee, J. Bae, Y. Kim, *J. Am. Chem. Soc.* **2018**, *140*, 11771–11776.
- [81] E. Thimsen, B. Sadtler, M. Y. Berezin, *Nat. Photonics* **2017**, *6*, 1043–1054.
- [82] S. Yu, D. Tu, W. Lian, J. Xu, X. Chen, *Sci. China Mater.* **2019**, *62*, 1071–1086.
- [83] A. Jain, A. Homayoun, C. W. Bannister, K. Yum, *Biotechnol. J.* **2015**, *10*, 447–459.
- [84] S. Diao, G. Hong, A. L. Antaris, J. L. Blackburn, K. Cheng, Z. Cheng, H. Dai, *Nano Res.* **2015**, *8*, 3027–3034.
- [85] N. M. Iverson, P. W. Barone, M. Shandell, L. J. Trudel, S. Sen, F. Sen, V. Ivanov, E. Atolia, E. Farias, T. P. McNicholas, *Nat. Nanotechnol.* **2013**, *8*, 873–880.
- [86] Z. Xue, S. Zeng, J. Hao, *Biomaterials* **2018**, *171*, 153–163.

Manuscript received: May 2, 2022

Revised manuscript received: October 8, 2022